Single-crystal and Molecular Structure, and Polarised Single-crystal Electronic-absorption and Electronic Spin Resonance Spectrum of Trichloro-oxobis[tris(dimethylamino)phosphine oxide]molybdenum(v)

By **C. David Garner,* Peter Lambert,** and **Frank E. Mabbs,** The Chemistry Department, Manchester University, Manchester M13 9PL
Trevor J. King, The Chemistry Department, Nottingham University, Nottingham NG7 2RD

The single-crystal structure of $[MoOCl_3\{P(NMe_2)_3O\}_2]$ has been determined by *X*-ray crystallography. The monoclinic unit cell of space group $P2_1/n$ with $a = 8.584(2)$, $b = 19.774(4)$, $c = 15.125(2)$ Å, and $\beta = 99.45(2)°$ contains four discrete molecules. These molecules have a distorted *mer*-octahedral geometry [Mo–O 1.686(5), Mo–Cl (mean) 2.373(17), Mo–O *trans* and *cis* to the oxo-group 2.169(4) and 2.056(5) Å respectively]. The polarised single-crystal electronic-absorption spectrum has been recorded from 10 000 to 30 000 cm^{-1} at room temperature and *ca.* 40 K. The single-crystal e.s.r. spectra of $[MoOCl_3\{P(NMe_2)_3O\}_2]$ as a pure compound and diluted in the isomorphous niobium analogue have been recorded at room temperature. The electronic structure of this d^1 system is discussed with reference to these structural and spectroscopic data.

ALTHOUGH a number of papers reporting aspects of the physical and chemical properties of mononuclear oxomolybdenum(v) compounds have been published,[1–13] no integrated and comprehensive study of the structure, spectra, and reactions of one particular species appears to have been accomplished. Here we report the preparation, single-crystal and molecular structure, polarised single-crystal electronic spectrum, and single-crystal e.s.r. spectrum of $[MoOCl_3\{P(NMe_2)_3O\}_2]$. The following paper [14] describes a study of the kinetics of the reactions of this compound with the nucleophiles Cl^-, Br^-, and $[NCS]^-$, and the oxidant $[NO_3]^-$.

EXPERIMENTAL

Syntheses.—Molybdenum pentachloride (Koch–Light) was purified by vacuum sublimation in a sealed tube over a temperature gradient of 290—25 °C. Tris(dimethylamino)-phosphine oxide (B.D.H.) was used without further purification. Absolute ethanol (James Burroughs, AnalaR grade) and acetone (normal commercial grade) were separately stored over degassed type 4A molecular sieves prior to use; MeCN and CH_2Cl_2 (Hopkin and Williams) were distilled over P_4O_{10} and CaH_2, respectively, before storing in a similar manner. All the preparations and recrystallisations were performed under an atmosphere of purified dinitrogen.

Trichloro-oxobis[tris(dimethylamino)phosphine oxide]-molybdenum(v). Molybdenum pentachloride (4.08 g, 14.9 mmol) and $P(NMe_2)_3O$ (6.0 g, 33.5 mmol) were dissolved separately in the minimum volume of ethanol and these solutions were then mixed. A bright green microcrystalline precipitate was obtained by partial evaporation of solvent under reduced pressure, yield 4.6 g (*ca.* 53%), m.p. 179—180 °C (decomp.) (Found: C, 25.0; H, 6.7; N, 14.5; P, 10.5; Mo, 16.9. Calc. for $C_{12}H_{36}Cl_3MoN_6O_3P_2$: C, 25.0; H, 6.3; N, 14.6; P, 10.7; Mo, 16.6%).

The compound $[NbOCl_3\{P(NMe_2)_3O\}_2]$ was prepared as described.[15]

Crystals of $[MoOCl_3\{P(NMe_2)_3O\}_2]$ suitable for *X*-ray crystallographic and single-crystal polarised electronic and e.s.r. spectral studies were obtained by the slow evaporation of acetone solutions of the compound. Crystals of $[NbOCl_3\{P(NMe_2)_3O\}_2]$, as the pure compound and containing *ca.* 1% of the molybdenum analogue, were prepared by evaporation of their respective MeCN solutions. *X*-Ray powder diffractometry showed that the compounds $[MOCl_3\{P(NMe_2)_3O\}_2]^-$ (M = Mo or Nb) obtained in this way are isomorphous and the unit-cell dimensions for the Nb–Mo derivative were indistinguishable from those of the pure molybdenum compound.

Single-crystal Structure.—Crystal data. $C_{12}H_{36}Cl_3MoN_6O_3P_2$, $M = 576.7$, Monoclinic $a = 8.584$ (2), $b = 19.774$ (4), $c = 15.125$ (2) Å, $\beta = 99.45(2)°$, $U = 2\,532$ Å^3, D_m (flotation) $= 1.49 \pm 0.02$ g cm^{-3}, $Z = 4$, $D_c = 1.51$ g cm^{-3}, $F(000) = 1\,188$, Mo-K_α radiation, $\lambda = 0.710\,7$ Å, μ(Mo-K_α) $= 9.7$ cm^{-1}. Space group $P2_1/n$ from systematic absences: $h0l$ for $h + l = 2n + 1$, $0k0$ for $k = 2n + 1$.

Preliminary unit-cell dimensions and space-group data were obtained from oscillation and Weissenberg photographs and refined on a Hilger and Watts four-circle diffractometer. The layers 0—11kl were explored for a needle-shaped crystal *ca.* 2 mm in length and 0.2 mm in cross-sectional diameter, and 3 833 reflections with $I > 3\sigma(I)$ in the range $0 < 2\theta < 55°$ were considered observed and used in the subsequent refinement. No account was taken of anomalous dispersion and no corrections were made for secondary extinction or absorption effects; the maximum error introduced by the neglect of absorption effects was estimated to be *ca.* 15% in F^2. Data-reduction and crystallographic calculations were carried out on the Nottingham I.C.L. 1906A computer using the Oxford University 'Crystals' programs. Atomic-scattering

[1] H. B. Gray and C. R. Hare, *Inorg. Chem.*, 1962, **1**, 363.
[2] C. R. Hare, U. Bernal, and H. B. Gray, *Inorg. Chem.*, 1962, **1**, 831.
[3] S. M. Horner and S. Y. Tyree, *Inorg. Chem.*, 1962, **1**, 122.
[4] R. A. D. Wentworth and T. S. Piper, *J. Chem. Phys.*, 1964, **41**, 3884.
[5] K. De Armond, B. B. Garrett, and H. G. Gutowsky, *J. Chem. Phys.*, 1965, **42**, 1019.
[6] P. C. H. Mitchell, *Quart. Rev.*, 1966, **20**, 103 and refs. therein.
[7] D. P. Rilema and C. H. Brubaker, jun., *Inorg. Chem.*, 1970, **9**, 397.
[8] E. A. Allen, B. J. Brisdon, D. A. Edwards, G. W. A. Fowles, and R. G. Williams, *J. Chem. Soc.*, 1963, 4649.
[9] H. Kon and N. E. Sharpless, *J. Phys. Chem.*, 1966, **70**, 105.
[10] P. T. Manoharan and M. T. Rogers, *J. Chem. Phys.*, 1968, **49**, 5510.
[11] I. N. Marov, *Proc. Conf. Chem. Uses Molybdenum*, University of Reading, 1973, ed. P. C. H. Mitchell, p. 63 and refs. therein.
[12] C. D. Garner, M. R. Hyde, F. E. Mabbs, and V. I. Routledge, *J.C.S. Dalton*, 1975, 1175, 1180.
[13] P. M. Boorman, C. D. Garner, and F. E. Mabbs, *J.C.S. Dalton*, 1975, 1299.
[14] C. D. Garner, M. R. Hyde, F. E. Mabbs, and V. I. Routledge, following paper.
[15] A. Baglahf, Ph.D. Thesis, University of Manchester, 1975.

factors were used as published.[16] The metal-atom positions were located from a three-dimensional Patterson synthesis, and subsequent Fourier syntheses clearly indicated the positions of all the light atoms, with the exception of those for the hydrogens. The atom positions and their anisotropic thermal parameters were then refined using least-squares procedures. A subsequent difference-Fourier synthesis revealed approximate positions for all the hydrogen atoms. Least-squares analyses including all the atoms with anisotropic temperature factors, using the weighting scheme $w = 1.0/\{1 + [F_o - B/A]\}^2$ with $A = 27.0$ and $B = 16.0$, converged at a conventional R value of 0.072. Structure factors and anisotropic thermal parameters are in Supplementary Publication No. SUP 22041 (35 pp.).*

Electronic-spectral Measurements.—Absorption spectra (10 000—40 000 cm^{-1}) were recorded as described earlier [17] for $[MoOCl_3\{P(NMe_2)_3O\}_2]$ dissolved in CH_2Cl_2 at room temperature and as suitably thinned crystals at room temperature and *ca.* 40 K. At room temperature the orientations of the crystals permitted measurement of the spectra with the electric vector of the incident beam polarised parallel to the crystallographic *a*, *b*, and *c** axes, and at 40 K

TABLE 1

Final positional parameters * for $[MoOCl_3\{P(NMe_2)_3O\}_2]$

Atom	*x/a*	*y/b*	*z/c*
Mo	0.094 31(8)	0.172 24(3)	0.198 27(4)
O(1)	0.060 2(7)	0.256 1(3)	0.188 3(4)
O(2)	0.075 4(6)	0.166 9(3)	0.331 9(3)
O(3)	0.139 2(6)	0.065 3(2)	0.222 1(3)
Cl(1)	0.125 1(3)	0.153 7(1)	0.048 4(1)
Cl(2)	0.372 5(3)	0.185 0(1)	0.241 4(2)
Cl(3)	−0.174 2(2)	0.137 0(1)	0.164 4(1)
P(1)	0.002 1(2)	0.191 5(1)	0.409 0(1)
P(2)	0.225 9(2)	−0.000 1(1)	0.218 0(1)
N(1)	−0.078 1(9)	0.266 2(3)	0.396 2(5)
N(2)	−0.140 2(9)	0.140 9(4)	0.422 9(5)
N(3)	0.141 9(9)	0.191 2(4)	0.495 4(4)
N(4)	0.362 4(8)	−0.006 6(3)	0.307 0(4)
N(5)	0.323 6(8)	−0.012 4(3)	0.134 9(4)
N(6)	0.094 1(7)	−0.060 0(3)	0.211 1(5)
C(1)	−0.009 2(15)	0.326 7(5)	0.437 5(9)
C(2)	−0.212 5(14)	0.277 7(6)	0.328 2(8)
C(3)	−0.269 0(14)	0.160 5(7)	0.468 0(10)
C(4)	−0.133 0(17)	0.070 0(5)	0.398 4(10)
C(5)	0.302 1(12)	0.207 9(7)	0.489 4(7)
C(6)	0.106 1(18)	0.192 7(9)	0.586 2(7)
C(7)	0.343 8(13)	0.028 8(5)	0.388 6(6)
C(8)	0.485 0(14)	−0.058 4(5)	0.321 9(8)
C(9)	0.466 1(12)	0.026 5(5)	0.132 4(7)
C(10)	0.234 1(12)	−0.030 2(5)	0.046 3(6)
C(11)	−0.072 1(12)	−0.048 9(5)	0.196 1(7)
C(12)	0.141 0(14)	−0.132 0(4)	0.212 6(9)

* The numbers in parentheses in this and subsequent Tables are the estimated standard deviations in the least significant digits.

data were obtained with the electric vector polarised parallel to the *b* and *c** axes.

Electron Spin Resonance Spectra.—Room-temperature e.s.r. spectra were recorded as previously described [18] on single crystals of $[MoOCl_3\{P(NMe_2)_3O\}_2]$ and for this compound diluted in the isomorphous niobium host. These crystals were mounted such that the magnetic field could be oriented in the *ab*, *bc**, and *ac** crystallographic planes.

RESULTS AND DISCUSSION

Crystal Structure.—The final atomic co-ordinates refined for $[MoOCl_3\{P(NMe_2)_3O\}_2]$ are listed in Table 1. The parameters refined for the hydrogen atoms are not included as they involve relatively larger errors. A representation of the crystal structure is shown in Figure 1. The structure comprises discrete molecular units

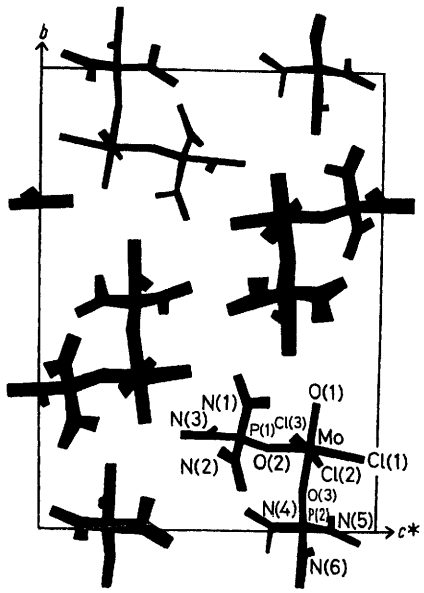

FIGURE 1 Crystal structure of $[MoOCl_3\{P(NMe_2)_3O\}_2]$ viewed down the *a* axis

oriented so that each oxomolybdenum(v) axis makes angles of 80.9, 10.4, and 85.0°, respectively, with the *a*, *b*, and *c** crystallographic axes. A diagram of the $[MoOCl_3\{P(NMe_2)_3O\}_2]$ molecule is presented in Figure 2, selected intramolecular dimensions are listed in Table 2, and Table 3 contains the equations of, and dihedral angles between, certain least-squares planes within the molecule. The co-ordination about the Mo^V is thus best described as a *mer*-distorted octahedral arrangement. The lengths of all the metal–ligand bonds [Mo=O 1.686(5), Mo–Cl 2.373(17) (mean), and Mo–P 2.056(5) and 2.169(4) Å] appear to be reasonable in view of data reported [19–21] for other related molybdenum compounds. The difference in the lengths of the Mo–O(P) bonds of 0.11 Å may be attributed to a structural *trans* effect exerted by the oxo-ligand, although this difference is smaller than that generally observed [19–21] for other oxomolybdenum centres. The six ligand donor atoms about the molybdenum approximately define an octahedron compressed along its *z* axis, with the metal atom

* For details see Notice to Authors No. 7, *J.C.S. Dalton*, 1976, Index issue.

[16] 'International Tables for *X*-Ray Crystallography,' Kynoch Press, Birmingham, 1962, vol. 3.

[17] D. L. McFadden, A. T. McPhail, C. D. Garner, and F. E. Mabbs, *J.C.S. Dalton*, 1975, 263.

[18] C. D. Garner, P. Lambert, F. E. Mabbs, and J. K. Porter, *J.C.S. Dalton*, 1972, 320.

[19] B. Spivack and Z. Dori, *Co-ordination Chem. Rev.*, 1975, **17**, 99 and refs. therein.

[20] P. M. Boorman, C. D. Garner, F. E. Mabbs, and T. J. King, *J.C.S. Chem. Comm.*, 1974, 663.

[21] C. D. Garner, L. H. Hill, F. E. Mabbs, D. L. McFadden, and A. T. McPhail, *J.C.S. Dalton*, 1977, 853.

displaced *ca.* 0.19 Å along this axis from the centroid of this polyhedron. The average values of the interbond angles subtended at the metal atom by adjacent pairs of donor atoms are: oxo-group with equatorial ligands, 95.8(1.3); equatorial ligand with equatorial ligand 89.4(1.4); and *trans*-oxygen with equatorial ligand, 84.2(3.3)°. The average ligand dimensions [O–P 1.498(5), P–N 1.629(8), N–C 1.446(14) Å; O–P–N 110.8(5.0), N–P–N 108.2(3.9), C–N–C 114.5(1.3), C–N–P 121.8(2.4)°] seem to be typical of values reported [22] for other $P(NMe_2)_3O$ compounds.

TABLE 2

Bond lengths (Å) and interbond angles (°) for $[MoOCl_3\{P(NMe_2)_3O\}_2]$

Co-ordination about Mo			
Mo–O(1)	1.686 (5)	O(1)–Mo–O(2)	95.6(3)
Mo–O(2)	2.056 (5)	O(1)–Mo–O(3)	175.6(2)
Mo–O(3)	2.169 (4)	O(1)–Mo–Cl(1)	96.5(2)
Mo–Cl(1)	2.353 (2)	O(1)–Mo–Cl(2)	94.1(2)
Mo–Cl(2)	2.383 (2)	O(1)–Mo–Cl(3)	97.0(2)
Mo–Cl(3)	2.382 (2)	O(2)–Mo–O(3)	80.0(2)
		O(2)–Mo–Cl(1)	167.9(2)
		O(2)–Mo–Cl(2)	88.5(2)
		O(2)–Mo–Cl(3)	88.1(2)
		O(3)–Mo–Cl(1)	87.9(1)
		O(3)–Mo–Cl(2)	85.1(1)
		O(3)–Mo–Cl(3)	83.7(1)
		Cl(1)–Mo–Cl(2)	90.8(1)
		Cl(1)–Mo–Cl(3)	90.3(1)
		Cl(2)–Mo–Cl(3)	168.7(1)
Phosphine groups			
P(1)–O(2)	1.495 (6)	O(2)–P(1)–N(1)	115.2(3)
P(2)–O(3)	1.500 (5)	O(2)–P(1)–N(2)	108.9(4)
average P–O	1.498 (5)	O(2)–P(1)–N(3)	106.5(4)
		O(3)–P(2)–N(4)	109.0(3)
P(1)–N(1)	1.629 (7)	O(3)–P(2)–N(5)	118.7(3)
P(1)–N(2)	1.619 (8)	O(3)–P(2)–N(6)	106.6(3)
P(1)–N(3)	1.622 (7)	average O–P–N	110.8(5.0)
P(2)–N(4)	1.638 (6)		
P(2)–N(5)	1.638 (7)	N(1)–P(1)–N(2)	105.3(4)
P(2)–N(6)	1.629 (6)	N(1)–P(1)–N(3)	108.8(4)
average P–N	1.629 (8)	N(2)–P(1)–N(3)	112.4(4)
		N(4)–P(2)–N(5)	103.4(3)
N(1)–C(1)	1.432 (12)	N(4)–P(2)–N(6)	113.0(3)
N(1)–C(2)	1.432 (13)	N(5)–P(2)–N(6)	106.3(4)
N(2)–C(3)	1.444 (17)	average N–P–N	108.2(3.9)
N(2)–C(4)	1.453 (13)		
N(3)–C(5)	1.424 (13)	C(1)–N(1)–C(2)	114.1(8)
N(3)–C(6)	1.456 (14)	C(3)–N(2)–C(4)	116.6(9)
N(4)–C(7)	1.449 (11)	C(5)–N(3)–C(6)	114.6(8)
N(4)–C(8)	1.460 (13)	C(7)–N(4)–C(8)	112.6(7)
N(5)–C(9)	1.450 (13)	C(9)–N(5)–C(10)	114.7(7)
N(5)–C(10)	1.474 (10)	C(11)–N(6)–C(12)	114.4(7)
N(6)–C(11)	1.424 (12)	average C–N–C	114.5(1.3)
N(6)–C(12)	1.478 (11)		
average N–C	1.446 (14)	C(1)–N(1)–P(1)	124.8(7)
		C(2)–N(1)–P(1)	120.3(6)
		C(3)–N(2)–P(1)	123.2(7)
		C(4)–N(2)–P(1)	119.9(8)
		C(5)–N(3)–P(1)	123.2(6)
		C(6)–N(3)–P(1)	121.1(8)
		C(7)–N(4)–P(2)	119.9(6)
		C(8)–N(4)–P(2)	125.5(6)
		C(9)–N(5)–P(2)	118.8(6)
		C(10)–N(5)–P(2)	118.5(6)
		C(11)–N(6)–P(2)	124.5(5)
		C(12)–N(6)–P(2)	121.0(6)
		average C–N–P	121.8(2.4)

[22] See, for example, J. F. de Wet and S. F. Darlow, *Inorg. Nuclear Chem. Letters*, 1971, **7**, 1041; J.-M. Le Carpentier, R. Schlupp, and R. Weiss, *Acta Cryst.*, 1972, **B28**, 1278; L. J. Radonovich and M. D. Glick, *J. Inorg. Nuclear Chem.*, 1973, **35**, 2745.

Electronic Spectrum.—The electronic-spectral data obtained are summarised in Table 4 and Figure 3. The first two bands in the room-temperature electronic spectrum at 13 000 and 22 500 cm^{-1} are similar in energy and intensity to those observed [23] for $[MoOX_5]^-$ (X = F, Cl, Br, or NCS), $[MoOCl_4]^-$, and $[MoOCl_4(OH_2)]^-$.[21] Fur-

TABLE 3

Equations [a] of some least-squares planes [b] and their dihedral angles for $[MoOCl_3\{P(NMe_2)_3\}_2]$

Plane (1): Mo, Cl(1), Cl(2), Cl(3), O(2)

$0.178\,4X - 0.977\,9Y + 0.108\,9Z + 2.767\,3 = 0$

[Mo −0.184 5, Cl(1) 0.044 0, Cl(2) 0.046 3, Cl(3) 0.046 0, O(1) −1.873 0, O(2) 0.048 4, O(3) 1.979 8, P(1) −0.448 9, P(2) 3.373 4]

Plane (2): Mo, O(1), O(3), Cl(2), Cl(3)

$-0.263\,7X - 0.088\,4Y + 0.960\,5Z - 3.102\,7 = 0$

[Mo −0.044 1, O(1) 0.030 7, O(3) 0.025 2, Cl(2) −0.006 0, Cl(3) −0.005 8, O(2) 1.991 3, Cl(1) −2.391 4, P(1) 3.356 4, P(2) −0.348 3]

Plane (3): Mo, O(1), O(2), O(3), Cl(1)

$-0.952\,7X - 0.182\,5Y - 0.242\,9Z + 1.644\,8 = 0$

[Mo 0.002 5, O(1) −0.008 9, O(2) 0.008 2, O(3) −0.008 5, Cl(1) 0.006 7, Cl(2) −2.372 5, Cl(3) 2.368 6, P(1) 0.422 0, P(2) −0.476 7]

Plane (4): P(1), N(1), C(1), C(2)

$0.684\,8X + 0.156\,6Y - 0.711\,7Z + 4.453\,2 = 0$

[P(1) 0.019 9, N(1) −0.061 7, C(1) 0.021 4, C(2) 0.020 4, O(2) 1.325 0, Mo 3.098 4]

Plane (5): P(1), N(2), C(3), C(4)

$-0.376\,8X + 0.237\,3Y - 0.895\,4Z + 4.177\,3 = 0$

[P(1) −0.012 2, N(2) 0.038 2, C(3) −0.013 3, C(4) −0.012 7, O(2) 0.593 5, Mo 2.217 5]

Plane (6): P(1), N(3), C(5), C(6)

$-0.142\,4X + 0.989\,7Y + 0.015\,4Z - 3.960\,6 = 0$

[P(1) 0.022 6, N(3) −0.069 9, C(5) 0.024 2, C(6) 0.023 1, O(2) −0.593 9, Mo −0.589 4]

Plane (7): P(2), N(4), C(7), C(8)

$0.649\,2X + 0.696\,2Y - 0.306\,5Z - 0.061\,0 = 0$

[P(2) −0.029 9, N(4) 0.091 0, C(7) −0.029 7, C(8) −0.031 4, O(3) 0.361 8, Mo 1.731 4]

Plane (8): P(2), N(5), C(9), C(10)

$-0.359\,4X + 0.890\,9Y - 0.277\,8Z + 1.467\,5 = 0$

[P(2) 0.059 2, N(5) −0.187 3, C(9) 0.064 8, C(10) 0.063 4, O(3) 1.466 3, Mo 3.565 8]

Plane (9): P(2), N(6), C(11), C(12)

$0.131\,4X - 0.005\,9Y - 0.991\,3Z + 3.049\,3 = 0$

[P(2) 0.009 3, N(6) −0.028 6, C(11) 0.010 0, C(12) 0.009 3, O(3) −0.159 2, Mo 0.138 7]

Dihedral angles (°) between planes

Plane	1	2	3	4	5	6	7	8
2	91.66							
3	91.03	89.89						
4	96.23	148.26	120.54					
5	113.37	137.70	57.78	65.39				
6	172.55	81.96	92.79	87.33	74.06			
7	126.75	113.84	132,15	39.49	78.76	53.71		
8	164.92	95.35	75.68	84.77	53.45	21.79	61.83	
9	94.52	170.88	83.30	37.38	33.20	92.28	67.35	77.12

[a] These equations are referred to the *a*, *b*, and *c** crystal axes and *X*, *Y*, and *Z* are in Å. [b] The perpendicular distances (Å) of certain atoms from a particular plane are given in square brackets.

[23] C. D. Garner, I. H. Hillier, F. E. Mabbs, and M. F. Guest, *Chem. Phys. Letters*, 1975, **32**, 224 and refs. therein.

thermore, approximating the polarisation of the electric vector parallel to the a, b, and c^* crystallographic axes to polarisation parallel to the x, z, and y molecular axes,

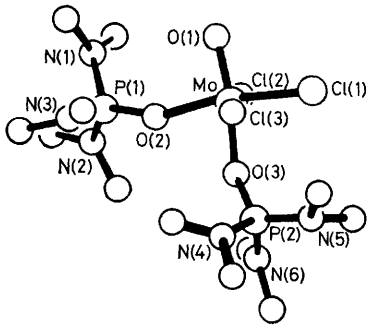

FIGURE 2 Structure of $[MoOCl_3\{P(NMe_2)_3O\}_2]$ molecules

respectively (Figures 1 and 6), the sense of the polarisation (y, $x \gg z$) is the same as that observed for $[AsPh_4][MoOCl_4]$, $[AsPh_4][MoOCl_4(OH_2)]$,[21] and $[AsPh_4][CrOCl_4]$.[24] Crystals of these latter compounds contain the metal atoms on sites of $\bar{4}$ symmetry and thus molecular C_{4v} symmetry is applicable for these chromophores, whereas it can only be an approximation for $[MoOCl_3\{P(NMe_2)_3O\}_2]$. The ligand donor atoms form a distorted octahedral array about the metal, the principal distortions being along the molecular z axis. Furthermore, the spectrochemical differences between

TABLE 4

Electronic absorption spectra for $[MoOCl_3\{P(NMe_2)_3O\}]$

Absorption maxima (10^3 cm^{-1}) *			
Single crystal			CH_2Cl_2 Solution
Room temperature	40 K		at room temperature
13.00 $x > y > z$	12.16	$y > z$	13.33 (20)
	12.99		
	13.77		
	14.50		
	15.25 (sh)		
22.50 $x > y > z$	22.80	$y > z$	22.47 (20)
			30.00 (sh) (*ca.* 1 400)
			34.00 (5 000)
			41.67 (6 000)

* Absorption coefficients (ε/dm^3 mol^{-1} cm^{-1}) are given in parentheses.

the chloride and phosphine ligands probably will be slight in comparison with such effects due to the oxo-group. Thus, it does not seem unreasonable to assume C_{4v} symmetry to be a good approximation in this case. Because of these features and the spectral similarities observed [23] for oxomolybdenum(v) compounds, it is anticipated that there is a common assignment for the two lowest-energy transitions of these compounds.

The assignment [21,23] of the lowest-energy absorption to the transition $b_2^*(4d_{xy}$, Mo–Cl $\pi^*) \rightarrow e^*(4d_{xz,yz}$, Mo–O $\pi^*)$ is consistent with earlier interpretations [1–10] of the spectra of oxomolybdenum(v) and related compounds. The fine structure resolved at low temperature for this band of $[MoOCl_3\{P(NMe_2)_3O\}_2]$ is similar to that obtained for $[MoOCl_4]^-$, $[MoOCl_4(OH_2)]^-$,[21] and $[CrOCl_4]^-$.[24] The first two components are separated by *ca.* 830 cm^{-1} and the other three separations average 750 $\pm$ 30 cm^{-1}. It seems possible that the first two

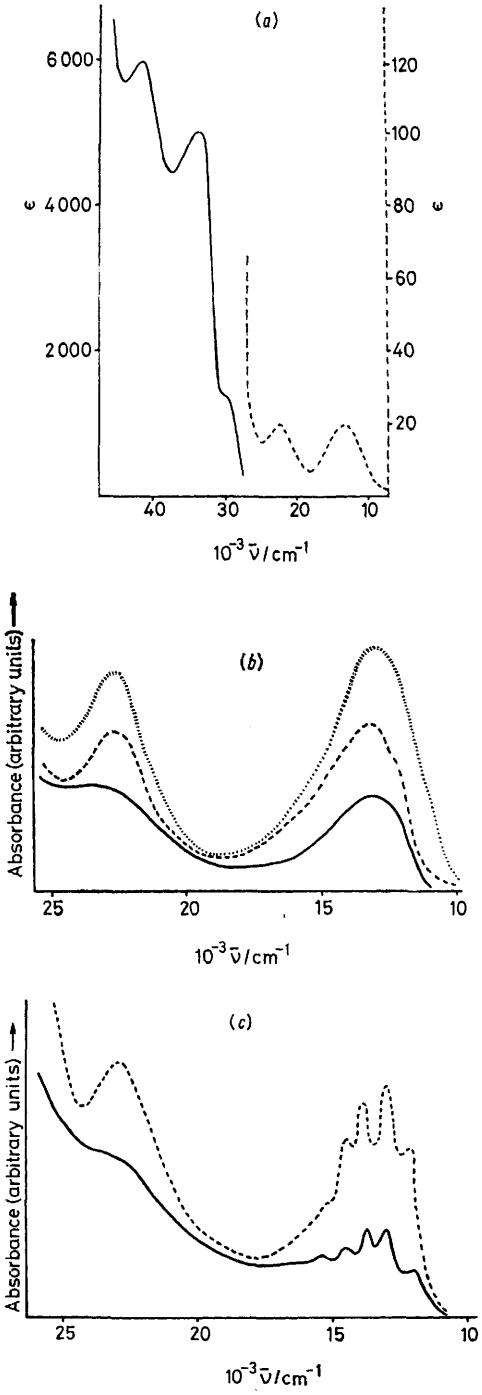

FIGURE 3 (*a*) Electronic spectrum of $[MoOCl_3\{P(NMe_2)_3O\}_2]$ in CH_2Cl_2 solution. (*b*) Polarised single-crystal spectra of $[MoOCl_3\{P(NMe_2)_3O\}_2]$ at room temperature, with the electric vector of the incident light parallel to the a (· · · ·), b (——), and c^* (– – – –) crystal axes. (*c*) Polarised single-crystal spectra of $[MoOCl_3\{P(NMe_2)_3O\}_2]$ at 40 K, with the electric vector of the incident light parallel to the b (——) and c^* (– – – –) crystal axes

[24] C. D. Garner, J. Kendrick, P. Lambert, F. E. Mabbs, and I. H. Hillier, *Inorg. Chem.*, 1975, **15**, 1287.

maxima at *ca.* 12 160 and 12 990 cm^{-1} represent two electronic origins for this $b_2^* \rightarrow e^*$ transition, the orbital degeneracy of the excited state being removed by spin–orbit coupling [21,24] and/or low-symmetry ligand-field effects. The average splitting of *ca.* 750 cm^{-1} is attributed to vibronic coupling with the ν(Mo–O) stretching mode. This frequency is less than the corresponding value of 996 cm^{-1} for the ground state, consistent with the transfer of an electron into an Mo–O π*-antibonding orbital.

The nature of the electronic transition responsible for the absorption at *ca.* 22 500 cm^{-1} is less straightforward. Gray and his co-workers [1,2] assigned this absorption to the transition $b_2^*(4d_{xy}$,Mo–Cl π*) → $b_1^*(4d_{x^2-y^2}$, Mo–Cl σ*). However, as discussed earlier,[23] the essential invariance of the energy of this transition to changes in the nature of the ligands *cis* to the oxo-group suggests that this explanation is incorrect. Furthermore, the *xy* polarisation of the transition, the comparable intensity of this and the electronically allowed $b_2^* \rightarrow e^*$ absorption, together with the rather similar and small reduction in intensity which occurs on cooling to low temperatures for both absorptions of each oxomolybdenum(V) compound studied, suggest that under C_{4v} symmetry the absorption at *ca.* 22 500 cm^{-1} is an electronically allowed $e \longleftrightarrow a$ or *b* transition. The nature of the fine structure resolved [21] for the transition at 22 500 cm^{-1} of $[MoOCl_4]^-$, *i.e.* series of maxima separated by *ca.* 340 cm^{-1}, the origin for the series in *z* polarisation being some 120 cm^{-1} lower in energy than that for the series in *xy* polarisation, also suggests a ^2E excited state which, in C_{4v}', has $\Gamma_7 < \Gamma_6$. Spin–orbit-coupling considerations show that such a splitting would arise for an e^3 configuration, but the reverse ($\Gamma_7 > \Gamma_6$) would occur for an e^1 configuration.

Therefore, these various considerations lead us to the conclusion that the second electronic transition of oxomolybdenum(V) compounds corresponds to a promotion of the type $e^4 \rightarrow a$ or *b*. There seem to be three possible assignments, e(O $2p_{x,y}$, Mo–O π) → $b_2^*(4d_{xy}$, Mo–Cl π*), → $b_1(4d_{x^2-y^2}$, Mo–Cl σ*), or → a_1^*-$(4d_{z^2}$, Mo–O σ*). Earlier [21] we argued in favour of this last interpretation by analogy with $[CrOCl_4]^-$ for which *ab initio* calculations suggested [24] such an assignment for the second absorption in the electronic spectrum of this ion. However, consideration of the detailed position of the two lowest spectral transition energies, in conjunction with certain aspects of the dimensions of those chloro-oxomolybdenum(V) compounds for which accurate structural data are available (Table 5), calls this particular assignment into question for these compounds. The slight but significant increase in the Mo–O(oxo) separation from that in $[AsPh_4][MoCl_4]$ [21] to that in $[MoOCl_3\{P(NMe_2)_3O\}_2]$ is accompanied by a small decrease in the value of the O–Mo–L(*cis*) interbond angles. A reduction in the energy of the first transition parallels these structural changes, whereas the energy of the second transition remains remarkably constant.

TABLE 5

Energies of the two lowest absorptions together with interatomic dimensions for certain chloro-oxomolybdenum(V) compounds

Compound	E_1 / 10^3 cm^{-1}	E_2 / 10^3 cm^{-1}	Bond/Å: Mo–O	Bond/Å: Mo–Cl (mean)	Angle/° O–Mo–L(*cis*)	Ref.
$[AsPh_4][MoOCl_4]$	15.4	22.5	1.610 (10)	2.333 (8)	105.3(0.1)	21
$[MoOCl_3(SPPh_3)]$	15.3	23.0	1.647 (3)	2.324 (2)	106.1(5.9)	20
$K_2[MoOCl_5]$	13.7	22.4	1.67(4)	2.400 (25)	*a*	*b*
$[AsPh_4][MoOCl_4(OH_2)]$	13.2	22.8	1.672 (19)	2.359 (3)	99.0(9)	21
$[MoOCl_3\{P(NMe_2)_3O\}_2]$	13.0	22.5	1.686 (3)	2.369 (18)	95.8(1.3)	*c*

[a] Not published. [b] L.O. Atovmyan, O. A. Dyanchenko, and E. B. Lobkovskii, *J. Struct. Chem.*, 1971, **11**, 429. [c] This work.

Figure 4 contains a simple molecular-orbital (m.o.) diagram which attempts to represent the expected effect on the relative energies of certain Mo–O group orbitals

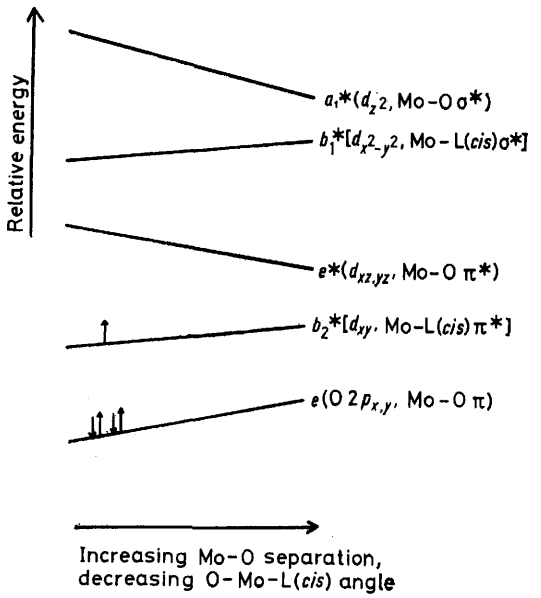

FIGURE 4 Suggested variation in the relative energies of certain orbitals associated with a mono-oxomolybdenum group as the Mo–O separation increases *and* the O–Mo–L(*cis*) interbond angles decrease

produced by a concomitant increase in Mo–O separation and a decrease in the O–Mo–L(*cis*) interbond angles. The observed reduction in the energy of the $b_2^*[4d_{xy}$, Mo–L(*cis*) π*] → $e^*(4d_{xz,yz}$, Mo–O π*) transition as the Mo–O separation increases and the O–Mo–L(*cis*) angles decrease is consistent with the diagram. Of the three assignments proposed above for the second absorption, the energies of the transitions e(O $2p_{x,y}$, Mo–O π) → $b_2^*(4d_{xy}$ Mo–Cl π*) and → $b_1^*(4d_{x^2-y^2}$, Mo–Cl σ*) are

expected to be less sensitive to changes in the Mo–O bond length and O–Mo–L(*cis*) interbond angles than is the promotion e(O $2p_{x,y}$, Mo–O π) $\rightarrow a_1(d_{z^2}$, Mo–O σ^*), which is expected to show an energy dependence on the structural dimensions similar to that described for the first transition. Therefore, of these assignments, the

The intense absorptions at *ca.* 34 000 and 42 000 cm^{-1} probably arise from ligand→metal charge-transfer transitions. The transition responsible for the shoulder at *ca.* 30 000 cm^{-1} appears to be relatively weak in its own right and thus it might be possible to ascribe this to a '*d–d*' electronic rearrangement. However, the general

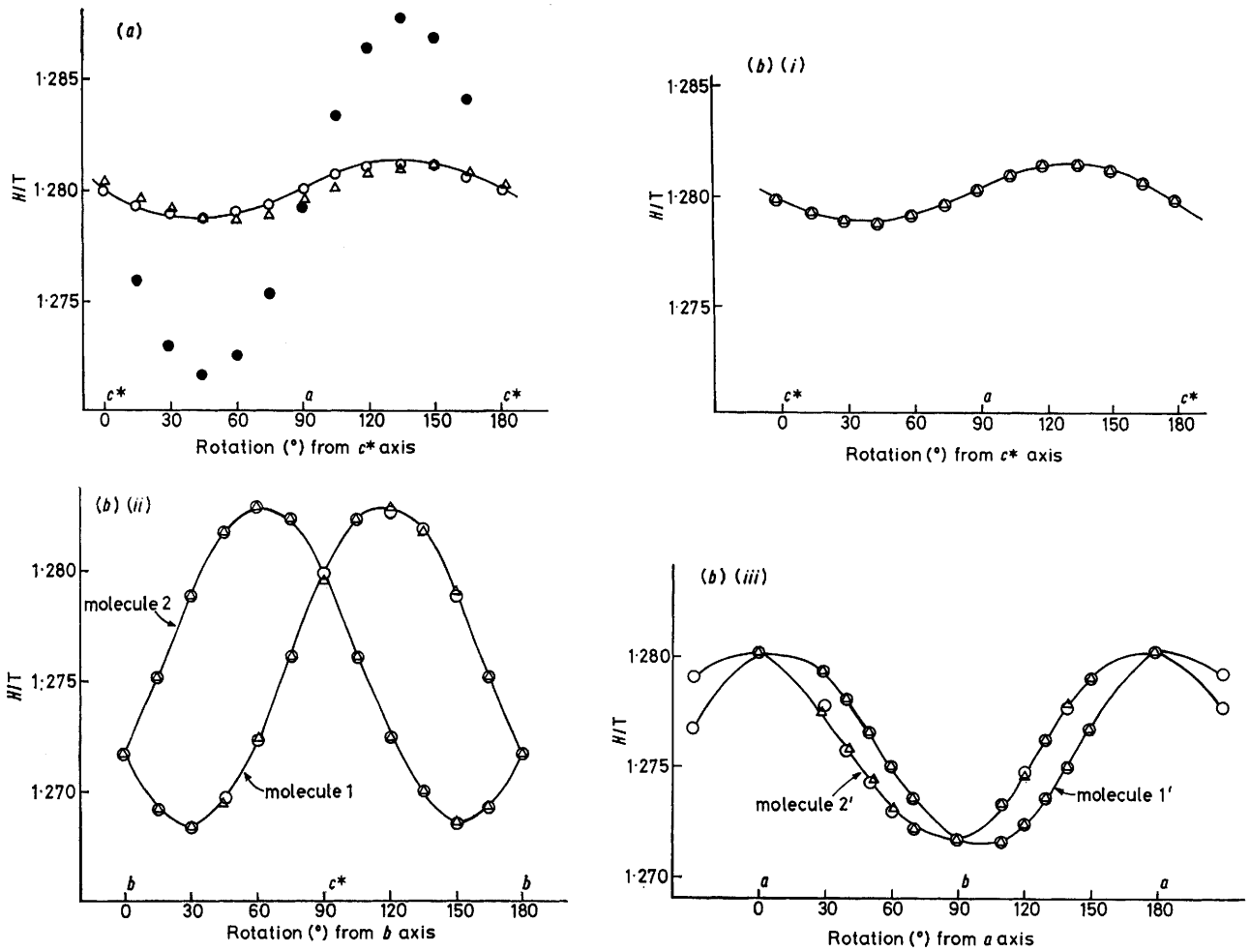

FIGURE 5 (*a*) E.s.r. data for $[MoOCl_3\{P(NMe_2)_3O\}_2]$ in the *ac** plane: (○) experimental data; (△) values calculated using assignment I; (●) values calculated using 'molecular' d.c.s with the *z* and *x* axes taken as the Mo–O and *ca.* Cl–Mo–Cl directions, respectively. (*b*) E.s.r. data recorded for $[(Nb,Mo)OCl_3\{P(NMe_2)_3O\}_2]$. (*i*) *ac** plane: (○) experimental data; (△) values calculated with $g^2 = 3.736\ 6 + 0.001\ 1\cos 2\theta + 0.007\ 6\sin 2\theta$. (*ii*) *bc** plane: (○) experimental data; (△) values calculated with $g^2 = 3.762\ 1 + 0.023\ 8\cos 2\theta + 0.035\ 9\sin 2\theta$ for molecule 1 and $g^2 = 3.761\ 8 + 0.023\ 9\cos 2\theta - 0.035\ 0\sin 2\theta$ for molecule 2. (*iii*) *ab* plane: (○) experimental values; (△) values calculated with $g^2 = 3.760\ 4 - 0.025\ 1\cos 2\theta + 0.005\ 6\sin 2\theta$ for molecule 1' and $g^2 = 3.761\ 0 - 0.025\ 3\cos 2\theta - 0.008\ 9\sin 2\theta$ for molecule 2'. All the data were recorded at 300 K with $\nu = 346.30$ MHz

$e \rightarrow a_1^*$ appears to be less likely than either the $e \rightarrow b_2^*$ or b_1^*. Since the $e \rightarrow b_1^*$ promotion energy almost certainly would be more sensitive to a change of the ligands in the series $[MoOX_5]^{2-}$ (X = F, Cl, Br, or NCS) than the $e \rightarrow b_2^*$ promotion, and the energy of this second transition shows [23] little dependence on the nature of X in this series, it is tentatively concluded that the second absorption of oxomolybdenum(v) compounds corresponds to the transition e(O $2p_{x,y}$, Mo–O π) $\rightarrow$ $b_2^*[4d_{xy}$, Mo–L(*cis*) $\pi^*]$. However, further studies are necessary to confirm this interpretation and to establish the detailed nature and origin of the vibrational fine structure accompanying [21,23] this electronic transition.

lack of detailed information available concerning the nature of electronic transitions above *ca.* 25 000 cm^{-1} in oxomolybdenum(v) compounds precludes any real debate of their origin.

E.S.R. Spectrum.—The information obtained by the use of e.s.r. spectroscopy for $[MoOCl_3\{P(NMe_2)_3O\}_2]$ as a pure compound and diluted in the isomorphous diamagnetic $[NbOCl_3\{P(NMe_2)_3O\}_2]$ host lattice is summarised in Tables 6 and 7 and Figure 5. In the pure compound, the expected signals from the two magnetically inequivalent molecules in the *ab* and *bc** planes were not observed, thus indicating significant intermolecular magnetic interaction. In such a magnetically

concentrated system, the single e.s.r. signal observed at any particular orientation occurs at a g value which is the mean of the g' values of the individual molecules in that orientation.[25] However, when the magnetic field is parallel to the crystallographic a, b, or c^* axes the molecules become equivalent and the observed g values are

$$\left.\begin{aligned} g_{aa}^2 &= g_1^2\alpha_1^2 + g_2^2\alpha_2^2 + g_3^2\alpha_3^2 \\ g_{bb}^2 &= g_1^2\beta_1^2 + g_2^2\beta_2^2 + g_3^2\beta_3^2 \\ g_{c^*c^*}^2 &= g_1^2\gamma_1^2 + g_2^2\gamma_2^2 + g_3^2\gamma_3^2 \end{aligned}\right\} \quad (1)$$

given by (1), where g_1, g_2, and g_3 are the principal molecular g values and α_i, β_i, and γ_i are their direction cosines, with respect to the a, b, and c^* axes, respectively. Thus the magnitudes of the principal molecular g values can be found if their direction cosines are known. To this purpose, an orthogonal set of principal molecular axes was obtained by assuming that one axis (z) lies along the Mo–O(oxo) bond and that another axis (x) is perpendicular to this direction and ' parallel ' to the Cl–Mo–Cl direction. Using the appropriate direction cosines and experimental values for g_{aa}, g_{bb}, and $g_{c^*c^*}$, we find that $g_z = g_x = 1.941$ and $g_y = 1.929$. These principal molecular g values and their direction cosines lead to a calculated angular variation of the e.s.r. spectrum which is in good agreement with the experimental observations (Figure 5) in the ab and bc^* planes, but which is in poor agreement for the ac^* plane. This failure to reproduce all the experimental data is taken to indicate that an incorrect orientation was assumed for the principal molecular g values.

TABLE 6

E.s.r. data for single crystals of $[MoOCl_3\{P(NMe_2)_3O\}_2]$ (ν = 346.30 MHz)

ab Plane, $b = 0$		bc^* plane, $b = 0$		ac^* plane, $c^* = 0$	
θ/°	$10H$/T	θ/°	$10H$/T	θ/°	$10H$/T
0	12.724	0	12.720	0	12.800
15	12.731	15	12.725	15	12.794
30	12.744	30	12.739	30	12.790
45	12.764	45	12.757	45	12.788
60	12.784	60	12.775	60	12.791
75	12.797	75	12.789	75	12.794
90	12.802	90	12.795	90	12.800
105	12.797	105	12.790	105	12.807
120	12.782	120	12.775	120	12.810
135	12.762	135	12.757	135	12.812
150	12.742	150	12.739	130	12.811
165	12.728	165	12.725	165	12.806
180	12.724	180	12.720	180	12.800

The e.s.r. spectra recorded for $[MoOCl_3\{P(NMe_2)_3O\}_2]$ diluted in the isomorphous niobium host resolved the magnetically inequivalent molecules in the ab and bc^* planes and molybdenum hyperfine structure was observed in all the three planes. The data obtained in this system were treated according to the methods of Schonland [26] and Lund and Vänngård [27] and the results are summarised in Table 7. These data were analysed and the two alternative interpretations shown reproduce the angular variation of the e.s.r. spectrum, observed for the pure compound, in all the three crystallographic planes. The details of the alternatives I and II are presented in Table 7 and they differ only in the orientation of the principal molecular g values, $g_1 = 1.928$ (7 for II), $g_2 = 1.932$ (4), and $g_3 = 1.951$ (0), with respect to the crystallographic, and therefore molecular, axes. Alternative I gives angles between the principal molecular g values and the molecular axes (defined as above), g_1 and y, g_2 and x, and g_3 and z of 22° 54′, 8° 6′, and 22° 48′, respectively, whereas II gives values of 46° 46′, 42° 58′, and 23° 22′, respectively. The calculated angular variation of the e.s.r. spectrum is identical for both alternatives in the ab and bc^* planes and 180° out of phase in the ac^* plane, with the calculated spectrum for alternative I having the same phase as that observed experimentally. This difference in phase corresponds to ambiguities in the relative signs of the off-diagonal elements of the g-tensor matrix in Schonland's [26] method and arises because of ambiguities in the handedness of the axis system when mounting and changing the orientation of the crystal. Thus, on these grounds, we cannot make a distinction between the two alternatives.

TABLE 7

Interpretations of the e.s.r. data for $[MoOCl_3\{P(NMe_2)_3O\}_2]$ diluted in $[NbOCl_3\{P(NMe_2)_3O\}_2]$

	Alternative I				Alternative II			
		direction cosines with respect to				direction cosines with respect to		
	g	a	b	c^*	g	a	b	c^*
g_1	1.928	0.200 5	0.438 8	−0.875 9	1.927	−0.429 9	0.435 5	−0.790 9
g_2	1.932	0.969 5	−0.217 3	0.113 1	1.934	0.901 9	0.166 1	−0.398 8
g_3	1.951	−0.140 7	−0.871 9	−0.469 0	1.950	−0.042 3	−0.884 7	−0.464 2
	A †				A †			
A_1	0.458 7	0.279 1	0.038 1	−0.959 5	0.422 1	0.602 1	−0.155 5	0.783 1
A_2	0.489 3	0.947 7	−0.171 8	0.268 9	0.527 3	−0.783 8	0.071 5	0.616 9
A_3	2.167 0	−0.154 6	−0.984 4	−0.084 1	2.165 5	−0.151 9	−0.985 3	−0.078 8

† × 10^4 cm^{-1}.

The data in Table 7 show that the principal axes of the g values and hyperfine tensors are not coincident. However, for assignment I, the axes of the hyperfine tensors are almost coincident with the molecular axes, the actual values being (between A_1 and y, A_2 and x, A_3 and z) 5° 0′, 1° 36′, and 3° 36′, respectively. To simplify the interpretation of the e.s.r. data, the following assumptions were made:

[25] D. M. S. Bagguley and J. H. E. Griffiths, *Proc. Roy. Soc.*, 1950, **A201**, 366.

[26] D. S. Schonland, *Proc. Phys. Soc.*, 1959, **73**, 788.

[27] A. Lund and T. Vänngård, *J. Chem. Phys.*, 1965, **42**, 2979.

(*i*) The *g* and *A* tensors identified for the diluted system are applicable to the pure compound.

(*ii*) Assignment I is the correct choice; the axes of the *A* tensor are coincident with the molecular *x*, *y*, and *z* axes. This leads to $|A_{xx}| = 36.21 \times 10^{-4}$, $|A_{yy}| = 35.09 \times 10^{-4}$, and $|A_{zz}| = 75.58 \times 10^{-4}$ cm^{-1}. In benzene and dichloromethane solutions $|\overline{A}| = 49.67 \times 10^{-4}$ cm^{-1}, thus indicating that the principal hyperfine-splitting constants all have the same sign.

(*iii*) g_2 and g_x are coincident and g_1 and g_3 lie in the molecular *yz* plane, g_3 making an angle of 22° with the *z* axis (Figure 6). The molecular *g* tensor is thus given by

$$\begin{pmatrix} g_{xx} & 0 & 0 \\ 0 & g_{yy} & g_{yz} \\ 0 & g_{zy} & g_{zz} \end{pmatrix} \qquad (2)$$

(2). The transformation which diagonalises this tensor is the solution in the *yz* plane given in (*iii*) and this results in $|g_{xx}| = 1.928$, $|g_{yy}| = 1.935$, $|g_{zy}| = |g_{yz}| = 0.176\ 8$, and $|g_{zz}| = 1.948$.

Using the above assumptions it is, in principle, possible to interpret these e.s.r. data for an $[MoOCl_3\{P(NMe_2)_3O\}_2]$ molecule of C_s symmetry, allowing for the mixing of the metal *d* functions and for metal–ligand orbital mixing, using a procedure similar to that of Abragam and Pryce.[28] However, the number of parameters, whose values are unknown but which are required to express the molecular *g* and *A* values in terms of the detailed electronic structure of the molecule, is far too large to permit any reliable interpretation of these quantities. Therefore, no such detailed analysis will be presented here. However, the form of the equations for g_{ij} and A_{ij} shows that the origin of the shift of the principal axes of the *g* tensor from the chosen molecular directions, and also the non-coincidence of the principal axes of the *g* and *A* tensors, have their origins in mixing between the various metal-based antibonding molecular orbitals allowed by the low symmetry.

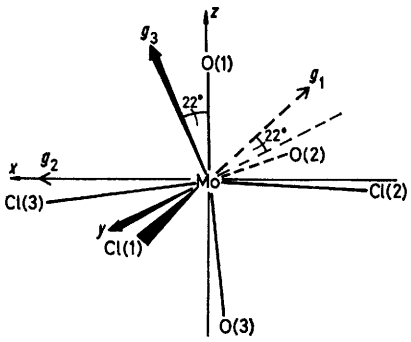

FIGURE 6 Orientation of molecular *g* values within the $[MoOCl_3\{P(NMe_2)_3O\}_2]$ molecule (assignment I)

We thank the S.R.C. for support.

[6/1867 *Received*, 5*th October*, 1976]

[28] A. Abragam and H. M. L. Pryce, *Proc. Roy. Soc.*, 1951, **A205**, 135.